A RELATION BETWEEN MASS AND RADIUS FOR 59 EXOPLANETS SMALLER THAN 4 EARTH RADII

Lauren M. Weiss[1,†] & Geoffrey W. Marcy[1]
[1]B-20 Hearst Field Annex, Astronomy Department, University of California, Berkeley, CA 94720
Draft version November 4, 2013

ABSTRACT

We study the masses and radii of 59 exoplanets smaller than $4R_\oplus$. We find a linear relation $M_P/M_\oplus = 0.21 + 2.78R_P/R_\oplus$. The RMS of planet masses to the linear fit is 3.8 $M_\oplus$, and our best fit has reduced $\chi^2 = 2.2$, indicating a large diversity in planet compositions below $4R_\oplus$. The exoplanets in our sample have orbital periods between 0 and 100 days. Wu & Lithwick (2013) find $M_P = 3R_P$ in 22 pairs of planets exhibiting transit timing variations, of which only 10 planets overlap with our sample. The linear mass-radius relation translates to a decrease in planet density with increasing radius ($M_P \propto \rho_P^{-2}$). We find that exoplanets have densities comparable to that of Earth at $1.6R_\oplus$; exoplanets smaller than $1.6R_\oplus$ are typically denser than Earth, indicating likely rocky compositions, whereas exoplanets larger than $1.6R_\oplus$ are typically less dense than Earth, indicating a significant fraction of H/He or water in their compositions.

1. INTRODUCTION

The Kepler Mission has found an abundance of planets with $R < 4R_\oplus$ (Batalha et al. 2013; **?**). However, in many systems, it is difficult to measure the masses of such small planets because the gravitational acceleration these planets induce on their host stars or neighboring planets is too small to detect with current telescopes and instruments. Obtaining measurements of the masses of these planets and characterizing their compositions is vital to understanding the formation and evolution of these planets.

Many scientists have explored the relation between planet mass and radius in the Solar system and beyond as a means for understanding exoplanet compositions (Lissauer et al. 2011; Enoch et al. 2012; Kane & Gelino 2012; Seager et al. 2007). Weiss et al. (2013) have shown that for planets between a few and 150 of Earth masses, we can predict the radius of a planet from its mass and incident stellar flux. However, below $4R_\oplus$, the large apparent scatter in planet mass impedes accurate predictions of planet mass. At $2R_\oplus$, planets are observed to span a decade in density, from less dense than water to densities suggesting a solid iron composition. One way to probe the scatter in planet mass is to attempt to measure the masses of more small planets.

2. SELECTING EXOPLANETS WITH MEASURED MASS AND RADIUS

Although uncertainties in the mass measurements for individual planets might be of order the planet mass, weak constraints on the masses of many small planets allow us to study the statistical distribution of planet masses for small planets. Marcy et al. (2013) measured the masses of 42 small, transiting planets. The planets were selected for their small size, and not based on predictions of their masses. Therefore, these 42 new transiting planets offer an unbiased survey of the masses of small planets. In this paper, we examine the relation between exoplanet mass and radius for the 40 exoplanets smaller than $4R_\oplus$ from Marcy et al. (2013), plus 19 exoplanets smaller than $4R_\oplus$ from the literature, for a total of 59 exoplanets. We also investigate how orbital parameters and stellar physical properties, including the planet's orbital period and semi-major axis, the incident flux from the star on the planet, and the stellar mass, radius, temperature, metallicity, and rotation, correlate with the residuals of the mass-radius relation.

2.1. *Including Mass Non-Detections for Statistical Soundness*

At a given radius, if we only include detections exceeding a certain confidence, we will preferentially include high-mass planets and will fail to include the low-mass planets that have comparable errors. This is especially true for small planets, for which the planet-induced RV signal ($\sim 1\,\mathrm{m\,s^{-1}}$) can be small compared to the noise from stellar activity ($\sim 5\,\mathrm{m\,s^{-1}}$). Although there is no physical reason that the stellar activity should phase with the orbit of a planet, random statistical fluctuations in the RVs can produce RVs that are high when they should be high, and low when they should be low, or the converse (RVs that are low when they should be high, and high when they should be low). Because RVs from stellar activity that phase with the expected planet signal will result in an over-estimate of planet mass, we must also include the RVs that are anti-phased with the expected planet signal. When Marcy et al. (2013) phase the RV measurements to the transit-determined planet ephemeris, they allow a negative semi-amplitude in the Keplerian fit to the RVs that results in a "negative" planet mass determination. Classically, these planets are considered non-detections, but we include them in the mass-radius relation to avoid statistical bias toward large planet masses at a given radius. Since there is no bias toward large or small planet masses in our sample, we can take the weighted mean mass of planets of a given radius and get a value representative of the planet population.

3. THE MASS-RADIUS RELATION FOR 59 SMALL EXOPLANETS

On average, exoplanet mass increases with increasing radius, indicating an underlying correlation in the individual exoplanet masses and radii. The individual measurements of planet mass and radius are shown in Figure 2 and listed in Table

We calculate the probability that mass and radius are uncorrelated for planets smaller than $4R_\oplus$. We calculate the correlation coefficient (Pearson R test) $r = 0.61$. In our sample of 59 exoplanets, the probability that these data are uncorrelated given $r = 0.61$ is 1.3×10^{-6}. Thus, the masses and radii of planets between the sizes of Earth and Neptune are correlated.

The individual masses and radii shown in Figure 2 suggest that exoplanet masses can be fit with a line. We verify this with a traditional power-law fit and obtain $M_P \propto R_P$ as the best result.

The weighted linear fit to the data for $R_P < 4R_\oplus$ is:

$$M_P/M_\oplus = -0.7 + 3.0 \, R_P/R_\oplus$$

There are 59 exoplanets in this sample. The reduced $\chi^2 = 2.2$, and the RMS $= 3.8M_\oplus$. The standard errors for the weighted linear fit are $slope = 3.0 \pm 0.6$, $intercept = -0.7 \pm 1.2$.

To illustrate how this population of exoplanets compares to our Solar System, we indicate the Solar System planets in Figure 2. A quadratic fit to the exoplanet population happens to line up with the Solar System planets, but has a reduced χ^2 that is twice as large as the linear fit to the exoplanets. Since most of the exoplanets in this sample have $P < 50$ days, we do not expect them to behave the same way as Uranus and Neptune, which have orbital periods of tens of thousands of days. Therefore, the hefty masses of Uranus and Neptune compared to planets of similar size that are closer to their stars is not unreasonable.

4. DISCUSSION

4.1. Interpretation of the Mass-Radius Relation

The correlation between exoplanet mass and radius for $R_P < 4R_\oplus$ indicates that Earth-size planets are less massive than Neptune-size planets.

The large reduced χ^2 values for the linear and quadratic mass-radius relations indicate that these relations are not sufficient models to explain the variation in planet mass at a given radius. A diversity of planet compositions, perhaps elucidated by correlation between the residuals and some other parameter, is required to explain the large scatter in planet mass.

The linear relation between planet mass and radius results in $\rho_P \propto R_P^{-2}$, indicating that planet density decreases strongly as mass and radius increase (see Figure 2). This can be attributed to an increasing fraction of volatiles with increasing planet mass.

The large fractional mass errors for $R_P < 1R_\oplus$ result in huge density errors. Although the planets smaller than $1R_\oplus$ do not have mass detections better than 2σ, their ensemble provides weak constraints on the expected mass of planets smaller than Earth. For instance, none of the planets smaller than Earth has a mass larger than $10M_\oplus$, and most have $M_P < 5M_\oplus$. Because we allow for negative planet masses in this regime, the weighted mean mass for planets between 0 and 1 $R_\oplus$ should not be statistically biased.

The reader might wonder if removing low-significance mass determinations would improve the robustness of the fit. In Figure 3, we use only the 42 exoplanets that have mass determinations of 1σ and better, which excludes most of the planets in the 0-1 $R_\oplus$ bin. The linear trend is still apparent, and the slope and intercept are similar to those in the less discriminating fit. However, we can see bias in this fit. The surviving small planets have larger masses than the discarded planets did, and so the intercept of the fit is higher, and the slope is shallower.

Previous work, including Lissauer et al. (2011) and Weiss et al. (2013), suggest that the mass-radius relation is more like $M_P \propto R_P^2$ for small exoplanets. However, these studies include Saturn or Saturn-like planets at the high-mass end of their populations. Such planets are better described as part of the giant planet population and are not useful in determining an empirical mass-radius relation for small exoplanets. Excluding Saturn-like planets gives a linear mass-radius relation for small planets.

In a study of planets with $M_P < 20M_\oplus$, Wu & Lithwick (2013) found $M_P/M_\oplus = 3R_P/R_\oplus$ in a sample of 22 pairs of planets that exhibited strong anti-correlated transit timing variations (TTVs). Our independent assessment of 59 planets, 49 of which are not analyzed in Wu & Lithwick (2013), agrees with this result.

Wu & Lithwick (2013) noted that a linear relation between planet mass and radius is dimensionally consistent with a constant escape velocity from the planet (i.e. $v_{esc}^2 \sim M_P/R_P$). The linear mass-radius relation might result from photo-evaporation of the atmospheres of small planets near their stars.

4.2. Interpretation of Planet Compositions

For detailed models of the compositions of the 42 new transiting planets presented in Marcy et al. (2013) and analyzed here, see Rogers (2013). Here, we consider the statistical properties of planet densities.

The densities of exoplanets with $R_P < 4R_\oplus$ and the densities binned by 1 $R_\oplus$ are shown in Figure 2. These data show that smaller planets have higher densities, and planets have an Earth-density at 1.6 $R_\oplus$. Planets smaller than 1.6 $R_\oplus$ tend to be denser than Earth, whereas planets larger than 1.6 $R_\oplus$ tend to be less dense than Earth. However, since rock and other materials are compressible, planets that are as dense as Earth but have larger radii are not necessarily solid rock; they need some lighter materials, such as water or a H/He envelope, to achieve the density of Earth.

4.3. Absence of Correlations with Mass and Radius Residuals

We examine the possibility that the residuals to the mass-radius relation correlate with some other parameters. We consider how the residual mass (exoplanet mass minus predicted mass), or, where more intuitive, residual radius (exoplanet radius minus predicted radius given the mass) correlates with various orbital properties and physical properties of the star. The quantities we consider are: planet orbital period, planet semi-major axis, the incident flux from the star on the planet, stellar mass, stellar radius, stellar temperature, stellar metallicity, stellar age, . The residual mass does not correlate

with any of these properties; the highest Pearson-R coefficient is 0.1. While we cannot rule out correlation between the mass residuals and other orbital and physical properties, we do not find evidence for any correlation to the residuals.

4.3.1. *A Weak Correlation between Residual Planet Mass and Stellar Metallicity*

The stellar metallicities of the stars in our sample are determined by spectroscopy and/or asteroseismology, yielding values accurate to 0.1 dex. We find a correlation between residual planet mass and stellar metallicity for planets smaller than $4R_\oplus$. The Pearson R-value of the correlation is 0.25, resulting in a probability of 5.8% that the residual planet mass and stellar metallicity are not correlated. In other words, we find a correlation between residual planet mass and metallicity with 2σ confidence in exoplanets smaller than $4R_\oplus$. In Figure 4, we plot residual planet mass and against stellar metallicity for the planets in our sample.

Buchhave et al. (2012) note that planets smaller than $4R_\oplus$ form around stars with a large range of metallicities. Their study includes 226 Kepler exoplanet candidates smaller than $4R_\oplus$, for which they obtained spectroscopic measurements of [m/H] in the host stars. Our work uses [Fe/H] as a metallicity indicator, and we are only considering validated exoplanets. Although Buchhave et al. (2012) find no relation between exoplanet occurrence and host star metallicity for $R_P < 4R_\oplus$, they do not comment on the relation between exoplanet size and host star metallicity for small planets. Therefore, our finding that planet mass correlates with stellar metallicity for $R_P < 4R_\oplus$ does not contradict their result.

5. CONCLUSIONS

For exoplanets with $R_P < 4R_\oplus$ and $P < 100$ days, planet radius correlates with planet mass with linear scaling, indicating that larger planets have substantially more volatiles than smaller planets. This relation is also different than the quadratic relation observed for the Solar System planets (excluding Jupiter). Uranus and Neptune are more massive than the exoplanets of their size in this sample, and they are also at much larger orbital distances than any of the exoplanets in our sample. A study of exoplanets of 3-4 $R_\oplus$ with orbital periods of dozens of years would better contextualize the mass and radius of Uranus and Neptune.

One reason Uranus and Neptune might be more massive than closer-in planets of the same size is that incident stellar flux might photo evaporate the atmospheres of closer-in counterparts, causing mass loss. The correlations between planet size and incident flux from the star for both large and small planets, and the absence of hot Neptunes, indicate that incident stellar flux of more than 100 times what Earth receives might play a key role in sculpting close-in planets.

Table 1
Exoplanets with Mass Upper Limits and $R_{\rm P} < 4R_\oplus$

| Name	Per (d)	Mass ($M_\oplus$)	Radius ($R_\oplus$)	Flux ($F_\oplus$)	First Ref.	Mass Ref.
55 Cnc e	0.737	8.38±0.39	2.21±0.15	2439.690	McArthur et al. (2004)	Endl et al. (2012)
CoRoT-7 b	0.854	5.02±0.86	1.68±0.09	1779.433	Queloz et al. (2009); Léger et al. (2009)	Queloz et al. (2009)
GJ 1214 b	1.580	6.26±0.91	2.80±0.24	16.631	Charbonneau et al. (2009)	Carter et al. (2011)
HD 97658 b	9.491	7.87±0.73	2.34±0.16	48.106	Howard et al. (2011)	Dragomir et al. (2013)
Kepler-10 b	0.837	4.54±1.25	1.42±0.03	3572.048	Batalha et al. (2011)	Batalha et al. (2011)
Kepler-11 b	10.304	1.90±1.20	1.80±0.04	126.512	Lissauer et al. (2011)	Lissauer et al. (2013)
Kepler-11 c	13.024	2.90±2.20	2.87±0.06	91.443	Lissauer et al. (2011)	Lissauer et al. (2013)
Kepler-11 d	22.684	7.30±1.10	3.12±0.07	43.563	Lissauer et al. (2011)	Lissauer et al. (2013)
Kepler-11 f	46.689	2.00±0.80	2.49±0.06	16.747	Lissauer et al. (2011)	Lissauer et al. (2013)
Kepler-18 b	3.505	6.90±3.48	2.00±0.10	462.244	Borucki et al. (2011)	Cochran et al. (2011)
Kepler-20 b	3.696	8.47±2.12	1.91±0.16	346.711	Borucki et al. (2011)	Gautier et al. (2012)
Kepler-20 c	10.854	15.73±3.31	3.07±0.25	82.445	Borucki et al. (2011)	Gautier et al. (2012)
Kepler-20 d	77.612	7.53±7.22	2.75±0.23	5.985	Borucki et al. (2011)	Gautier et al. (2012)
Kepler-36 b	13.840	4.46±0.30	1.48±0.03	217.365	Borucki et al. (2011)	Carter et al. (2012)
Kepler-36 c	16.239	8.10±0.53	3.68±0.05	175.646	Carter et al. (2012)	Carter et al. (2012)
Kepler-68 b	5.399	8.30±2.30	2.31±0.03	409.092	Borucki et al. (2011)	Gilliland et al. (2013)
Kepler-68 c	9.605	4.38±2.80	0.95±0.04	189.764	Batalha et al. (2013)	Gilliland et al. (2013)
Kepler-78 b	0.354	1.78±0.30	1.20±0.09	3093.388	Sanchis-Ojeda et al. (2013)	Howard et al. (2013, submitted)
KOI-94 b	3.743	9.40±4.50	1.77±0.17	1155.374	Batalha et al. (2013)	Weiss et al. (2013)
KOI-41.01	12.816	0.85±4.00	2.20±0.05	213.371	Borucki et al. (2011)	Marcy et al. (2013)
KOI-41.02	6.887	7.34±3.20	1.32±0.04	472.831	Borucki et al. (2011)	Marcy et al. (2013)
KOI-41.03	35.333	-4.36±4.10	1.61±0.05	55.812	Borucki et al. (2011)	Marcy et al. (2013)
KOI-69.01	4.727	2.59±2.00	1.50±0.03	220.120	Borucki et al. (2011)	Marcy et al. (2013)
KOI-82.01	16.146	8.93±2.00	2.22±0.07	17.278	Borucki et al. (2011)	Marcy et al. (2013)
KOI-82.02	10.312	3.80±1.80	1.18±0.04	31.184	Borucki et al. (2011)	Marcy et al. (2013)
KOI-82.03	27.454	0.62±3.30	0.88±0.03	8.250	Borucki et al. (2011)	Marcy et al. (2013)
KOI-82.04	7.071	-1.58±2.00	0.58±0.02	51.315	Borucki et al. (2011)	Marcy et al. (2013)
KOI-82.05	5.287	0.41±1.60	0.47±0.02	78.407	Borucki et al. (2011)	Marcy et al. (2013)
KOI-104.01	2.508	10.84±1.40	3.51±0.15	214.674	Borucki et al. (2011)	Marcy et al. (2013)
KOI-108.01	15.965	14.11±4.70	3.37±0.09	124.197	Borucki et al. (2011)	Marcy et al. (2013)
KOI-116.01	13.571	10.44±3.20	2.50±0.32	84.462	Borucki et al. (2011)	Marcy et al. (2013)
KOI-116.02	43.844	11.17±5.80	2.56±0.33	15.645	Borucki et al. (2011)	Marcy et al. (2013)
KOI-116.03	6.165	0.15±2.80	0.82±0.11	239.077	Borucki et al. (2011)	Marcy et al. (2013)
KOI-116.04	23.980	-6.39±7.00	0.95±0.13	43.146	Borucki et al. (2011)	Marcy et al. (2013)
KOI-122.01	11.523	13.00±2.90	3.42±0.09	182.708	Borucki et al. (2011)	Marcy et al. (2013)
KOI-123.01	6.482	1.30±5.40	2.37±0.07	444.879	Borucki et al. (2011)	Marcy et al. (2013)
KOI-123.02	21.223	2.22±7.80	2.52±0.07	94.934	Borucki et al. (2011)	Marcy et al. (2013)
KOI-148.01	4.778	3.94±2.10	1.88±0.10	168.932	Borucki et al. (2011)	Marcy et al. (2013)
KOI-148.02	9.674	14.61±2.30	2.71±0.14	225.109	Borucki et al. (2011)	Marcy et al. (2013)
KOI-148.03	42.896	7.93±4.60	2.04±0.11	13.545	Borucki et al. (2011)	Marcy et al. (2013)
KOI-153.01	8.925	-4.60±6.20	2.19±0.06	50.981	Borucki et al. (2011)	Marcy et al. (2013)
KOI-153.02	4.754	7.10±3.30	1.82±0.05	63.986	Borucki et al. (2011)	Marcy et al. (2013)
KOI-244.02	6.239	9.60±4.20	2.71±0.05	667.269	Borucki et al. (2011)	Marcy et al. (2013)
KOI-245.01	39.792	1.87±9.08	1.94±0.06	7.710	Borucki et al. (2011)	Marcy et al. (2013)
KOI-245.02	21.302	3.35±4.00	0.75±0.03	16.291	Borucki et al. (2011)	Marcy et al. (2013)
KOI-245.03	13.367	2.78±3.70	0.32±0.04	37.373	Borucki et al. (2011)	Marcy et al. (2013)
KOI-246.01	5.399	5.97±1.70	2.33±0.02	375.530	Borucki et al. (2011)	Marcy et al. (2013)
KOI-246.02	9.605	2.18±3.50	1.00±0.02	220.199	Borucki et al. (2011)	Marcy et al. (2013)
KOI-261.01	16.238	8.46±3.40	2.67±0.22	73.950	Borucki et al. (2011)	Marcy et al. (2013)
KOI-283.01	16.092	16.13±3.50	2.41±0.20	71.656	Borucki et al. (2011)	Marcy et al. (2013)
KOI-283.02	25.517	8.25±5.90	0.84±0.07	28.891	Borucki et al. (2011)	Marcy et al. (2013)
KOI-292.01	2.587	3.51±1.90	1.48±0.13	851.551	Borucki et al. (2011)	Marcy et al. (2013)
KOI-299.01	1.542	3.55±1.60	1.99±0.22	1581.816	Borucki et al. (2011)	Marcy et al. (2013)
KOI-305.01	4.604	6.15±1.30	1.48±0.08	90.372	Borucki et al. (2011)	Marcy et al. (2013)
KOI-321.01	2.426	6.35±1.40	1.43±0.03	713.204	Borucki et al. (2011)	Marcy et al. (2013)
KOI-321.02	4.623	2.71±1.80	0.85±0.03	291.503	Borucki et al. (2011)	Marcy et al. (2013)
KOI-1442.01	0.669	0.06±1.20	1.07±0.02	3645.770	Borucki et al. (2011)	Marcy et al. (2013)
KOI-1612.01	2.465	0.48±3.20	0.82±0.03	1691.964	Borucki et al. (2011)	Marcy et al. (2013)
KOI-1925.01	68.958	2.69±6.20	1.19±0.03	6.165	Borucki et al. (2011)	Marcy et al. (2013)
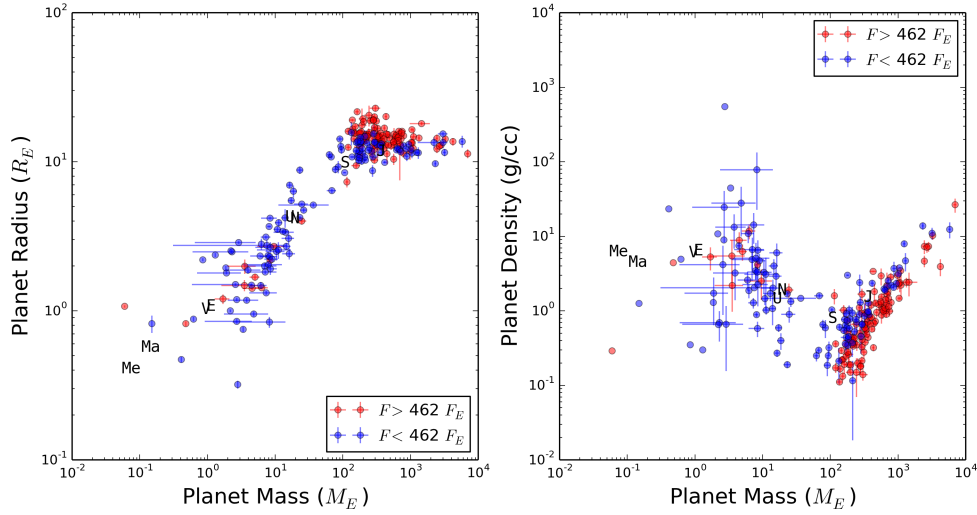
Figure 1. Left: Radius vs. mass for 243 exoplanets with measured masses and radii. Below $150 M_\oplus$, planet radius increases with planet mass; above $150 M_\oplus$, planet radius slightly decreases with planet mass. The solar system planets are shown as black triangles for comparison. Planets receiving lower than the median incident flux in this sample (462 times the incident flux at Earth) are blue; those receiving higher than the median incident flux are red. For giant planets (above about $150 M_\oplus$), planet radius increases with increasing incident flux, whereas for the smaller planets, the relation between radius and incident flux is uncertain. **Right:** Density vs. mass for 243 exoplanets with measured masses and radii. The break at $150 M_\oplus$ separates the low-mass planets, for which density decreases with increasing mass, from the high-mass planets, for which density increases with increasing mass. The flux coloration is the same as the left figure.
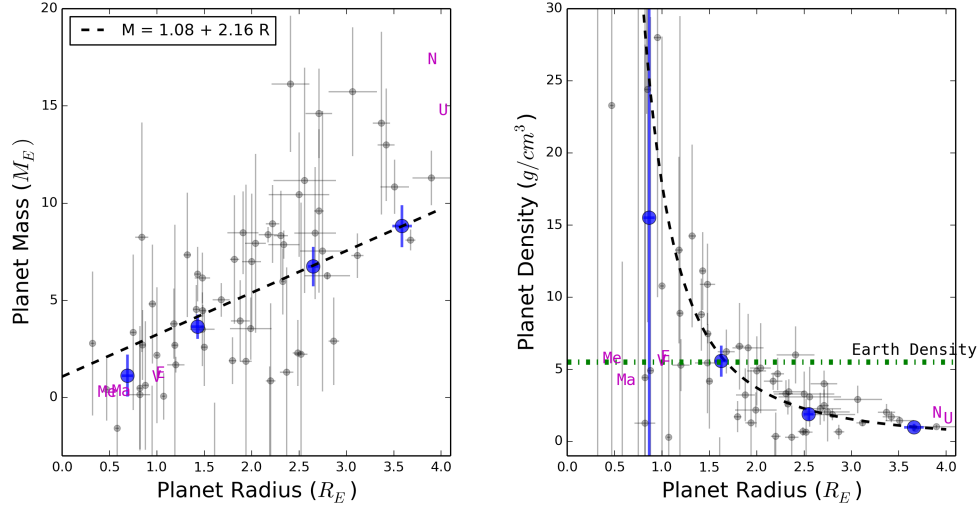
Figure 2. Planet mass vs. radius (left) and density vs. radius (right) for 59 exoplanets with measured mass and radius. The small gray points are mass-radius measurements and 1σ error bars. The black dashed line is the weighted linear fit to the data: $\frac{M_\mathrm{P}}{M_\oplus} = 1.08 + 2.16\frac{R_\mathrm{P}}{R_\oplus}$. The large blue points are the weighted mean exoplanet mass and density in bins of 1 Earth radius, with error bars representing the uncertainty in the means. The magenta squares are solar system planets Mercury, Venus, Earth, Mars, Uranus, and Neptune. The weighted means and the solar system planets are to guide the eye only; they were not used in calculating the linear fit. In the right plot, Earth's density ($5.5\,\mathrm{g\,cm^{-3}}$) is demarcated with a dotted green line. Note that all of the planets smaller than Earth have $M_\mathrm{P} < 10 M_\oplus$, and most of them have masses in the range $0 < M_\mathrm{P}/M_\oplus < 5$. Although none of these planets constitutes a 2σ mass detection individually, as an ensemble, they offer information about the typical mass for planets between 0 and 1 Earth radii.
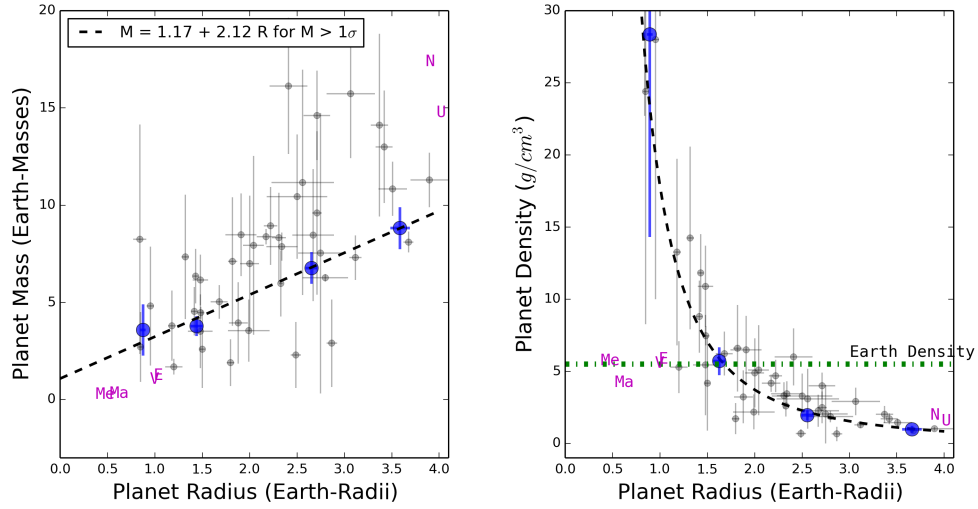
Figure 3. Planet mass vs. radius (left) and density vs. radius (right) for 42 exoplanets with measured radius and mass such that $M_P > 1\sigma$. The small gray points are mass-radius measurements for $M_P > 1\sigma$ and 1σ error bars. The black dashed line is the weighted linear fit to the data: $\frac{M_P}{M_\oplus} = 1.17 + 2.12\frac{R_P}{R_\oplus}$. Note that this fit is different from the best fit derived from all the data (see Figure 2). By only considering masses determined to better than 1σ, we are systematically excluding the low-mass planets at small radii (especially in the 0-1 $R_\oplus$ bin), thereby biasing our data toward larger planet masses. The linear fit reveals this bias: the y-intercept is higher and the slope is lower, indicating that we have removed the low-mass, small planets from our sample.
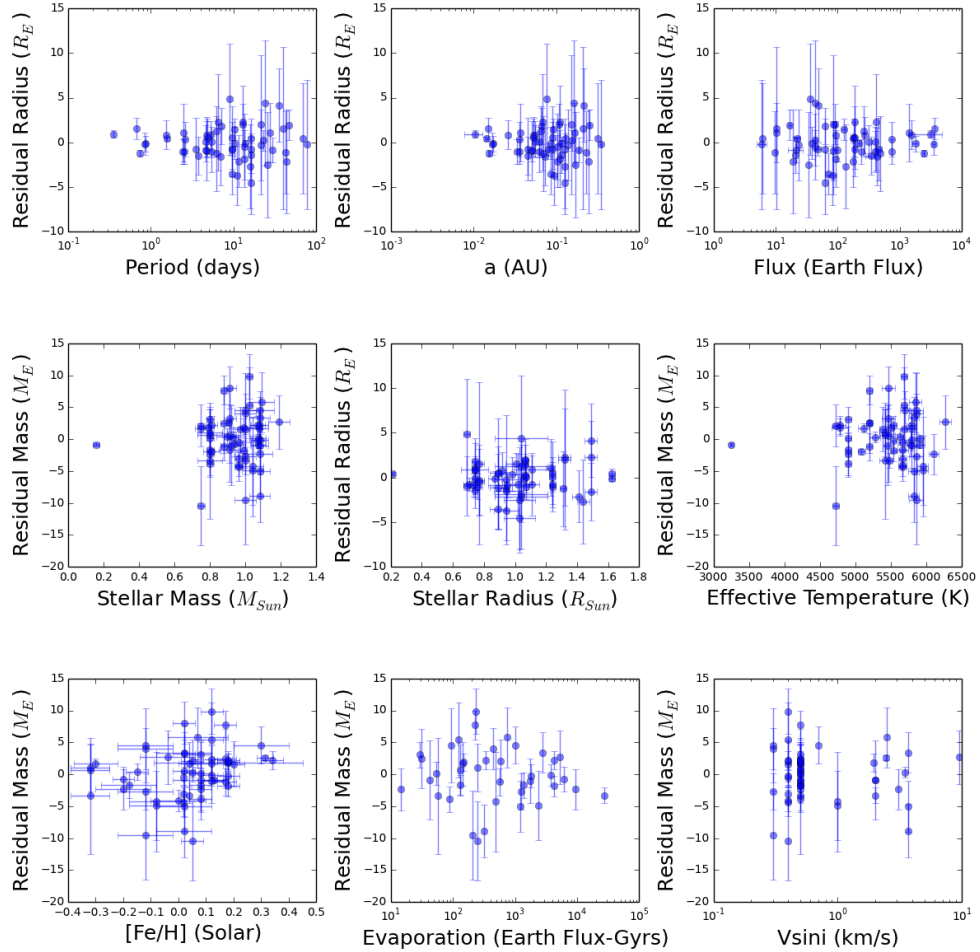
Figure 4. Mass and radius residuals (measured minus predicted mass or radius) versus various orbital and stellar properties for planets with $R_P < 4R_\oplus$ and 1σ uncertainties. There is a weak correlation (R=0.25, 2σ confidence) between residual mass and stellar metallicity (bottom left); none of the other residuals show correlation. The spread of the residuals is higher at long orbital periods and orbital distances than at short orbital periods and orbital distances (top row), indicating a possibly larger diversity of exoplanet compositions at large orbital distances than close-in.

REFERENCES

Batalha, N. M., Borucki, W. J., Bryson, S. T., et al. 2011, ApJ, 729, 27

Batalha, N. M., Rowe, J. F., Bryson, S. T., et al. 2013, ApJS, 204, 24

Borucki, W. J., Koch, D. G., Basri, G., et al. 2011, ApJ, 736, 19

Buchhave, L. A., Latham, D. W., Johansen, A., et al. 2012, Nature, 486, 375

Carter, J. A., Winn, J. N., Holman, M. J., et al. 2011, ApJ, 730, 82

Carter, J. A., Agol, E., Chaplin, W. J., et al. 2012, Science, 337, 556

Charbonneau, D., Berta, Z. K., Irwin, J., et al. 2009, Nature, 462, 891

Cochran, W. D., Fabrycky, D. C., Torres, G., et al. 2011, ApJS, 197, 7

Dragomir, D., Matthews, J. M., Eastman, J. D., et al. 2013, ApJ, 772, L2

Endl, M., Robertson, P., Cochran, W. D., et al. 2012, ApJ, 759, 19

Enoch, B., Collier Cameron, A., & Horne, K. 2012, A&A, 540, A99

Gautier, III, T. N., Charbonneau, D., Rowe, J. F., et al. 2012, ApJ, 749, 15

Gilliland, R. L., Marcy, G. W., Rowe, J. F., et al. 2013, ApJ, 766, 40

Howard, A. W., Johnson, J. A., Marcy, G. W., et al. 2011, The Astrophysical Journal, 726, 73

Kane, S. R., & Gelino, D. M. 2012, PASP, 124, 323

Léger, A., Rouan, D., Schneider, J., et al. 2009, A&A, 506, 287

Lissauer, J. J., Fabrycky, D. C., Ford, E. B., et al. 2011, Nature, 470, 53

Lissauer, J. J., Jontof-Hutter, D., Rowe, J. F., et al. 2013, ApJ, 770, 131

Marcy, G. W., Isaacson, H., & Rowe, J. F. 2013, in prep.

McArthur, B. E., Endl, M., Cochran, W. D., et al. 2004, ApJ, 614, L81

Queloz, D., Bouchy, F., Moutou, C., et al. 2009, A&A, 506, 303

Rogers, L. 2013, in prep.

Sanchis-Ojeda, R., Rappaport, S., Winn, J. N., et al. 2013, ApJ, 774, 54

Seager, S., Kuchner, M., Hier-Majumder, C. A., & Militzer, B. 2007, ApJ, 669, 1279

Weiss, L. M., Marcy, G. W., Rowe, J. F., et al. 2013, ApJ, 768, 14

Wu, Y., & Lithwick, Y. 2013, ApJ, 772, 74